

Evolution of plasmonic nanostructures under ultra-low-energy ion bombardment

Supplementary Material

Lionel Simonot^{a,*}, Florian Chabanais^{a,1}, Sophie Rousselet^a, Frédéric Pailloux^a,
Sophie Camelio^a, David Babonneau^{a,*}

^a*Institut Pprime, Département Physique et Mécanique des Matériaux, UPR 3346 CNRS,
Université de Poitiers, SP2MI, TSA 41123, Cedex 9, 86073 Poitiers, France*

1. Self-organized Ag nanoparticle chains

1.1. Atomic force microscopy

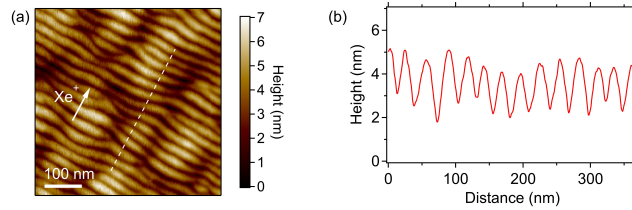


Figure S1: Atomic force microscopy of the nanorippled alumina surface obtained after 1 keV Xe^+ -ion exposure at oblique incidence. (a) False color topographic image (the projection of the ion beam direction onto the surface is indicated by the white arrow), and (b) height profile along the dotted line.

*Corresponding author

Email addresses: lionel.simonot@univ-poitiers.fr (Lionel Simonot),
david.babonneau@univ-poitiers.fr (David Babonneau)

¹Now at Normandie Univ, UNIROUEN, INSA Rouen, CNRS, Groupe de Physique des Matériaux, 76000 Rouen, France.

1.2. Finite-difference time-domain calculations

In addition to far-field optical measurements, numerical simulations were performed by finite-difference time-domain (FDTD) calculations using the FDTD Solutions software purchased from Lumerical (<http://www.lumerical.com/tcad-products/fdtd/>). We considered an assembly of identical ellipsoidal Ag nanoparticles with in-plane dimensions and gaps corresponding to the average experimental values, as determined by HAADF-STEM analysis (Table 1). The dielectric functions of the materials were determined from ellipsometric measurements of 100-nm thick alumina and Ag films grown by ion-beam deposition at room temperature. We used periodic boundary conditions in both the longitudinal and transverse directions, while perfectly matched layer boundary conditions were applied in the z direction. The height of the Ag nanoparticles, H , was then adjusted in order to fit the spectral position of the experimental surface plasmon resonance for a transverse excitation.

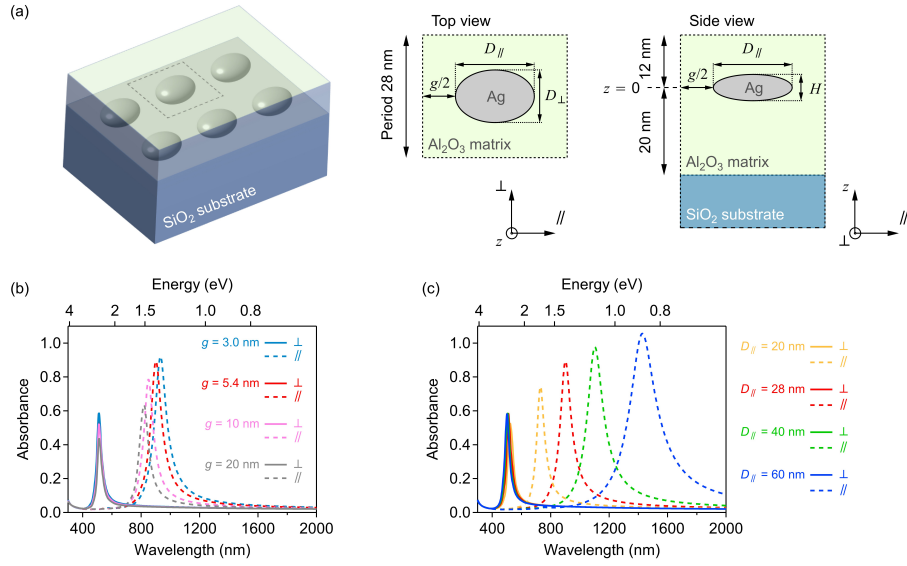


Figure S2: (a) Sketch of the configuration used to perform FDTD calculations for self-organized Ag nanoparticle chains surrounded by an alumina matrix deposited on a fused silica substrate. Absorption spectra calculated by FDTD method using the morphological parameters gathered in Table 1 for $t_{\text{sput}} = 0$ s ($H = 5.0$ nm): (b) Influence of the interparticle gap g and (c) of the in-plane diameter in the longitudinal direction D_{\parallel} .

1.3. Transmission electron microscopy and optical measurements

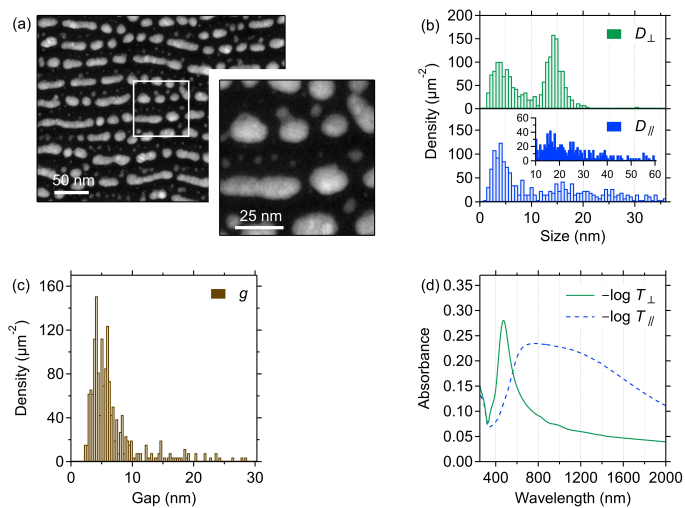


Figure S3: Self-organized Ag nanoparticles grown on rippled alumina thin films with 80 eV Ar^+ -ion bombardment at normal incidence for 60 s before alumina capping-layer deposition. (a) Plane-view HAADF-STEM image with a zoomed area indicated by the white rectangle, (b) in-plane size distributions in the longitudinal (D_{\parallel}) and transverse (D_{\perp}) directions, (c) distribution of interparticle gaps (g), and (d) corresponding absorbance spectra collected with longitudinal and transverse polarizations of the incident light.

2. Si₃N₄ layer

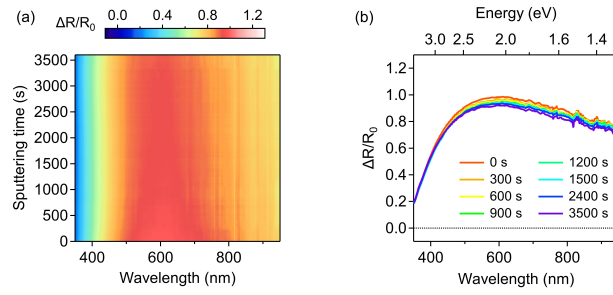


Figure S4: (a) Map of the SDRS signal $\Delta R(\lambda, t_{\text{sput}})/R_0$ collected during 80 eV Ar⁺-ion bombardment at normal incidence on a 92-nm thick Si₃N₄ layer deposited at room temperature by reactive magnetron sputtering. (b) Corresponding SDRS spectra for different sputtering durations t_{sput} .

3. Quasi-continuous Ag layer

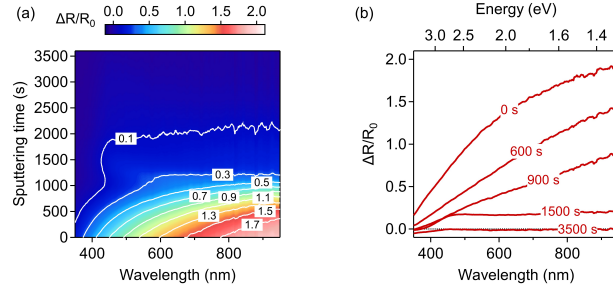


Figure S5: (a) Map of the SDRS signal $\Delta R(\lambda, t_{\text{sput}})/R_0$ collected during 80 eV Ar^+ -ion bombardment at normal incidence on an initially quasi-continuous Ag layer grown on Si_3N_4 (12.8 nm effective thickness). (b) Corresponding SDRS spectra for different sputtering durations t_{sput} .

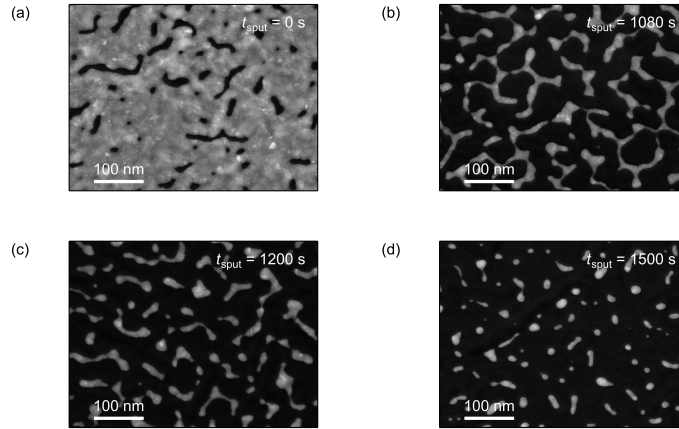


Figure S6: Plane-view HAADF-STEM images for $\text{Si}_3\text{N}_4:\text{Ag}:\text{Si}_3\text{N}_4$ trilayers corresponding to different sputtering durations t_{sput} of an initially quasi-continuous Ag layer (12.8 nm effective thickness) subjected to 80 eV Ar^+ -ion bombardment at normal incidence. (a) $t_{\text{sput}} = 0$ s, (b) $t_{\text{sput}} = 1080$ s, (c) $t_{\text{sput}} = 1200$ s, and (d) $t_{\text{sput}} = 1500$ s.

4. Coalescing Ag nanoparticles with short-range order

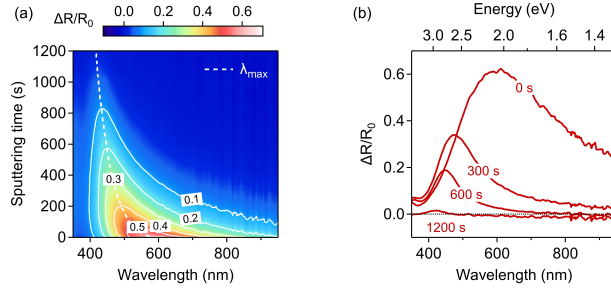


Figure S7: (a) Map of the SDRS signal $\Delta R(\lambda, t_{\text{sput}})/R_0$ collected during 80 eV Ar^+ -ion bombardment at normal incidence on an initially Ag nanoparticle layer grown on Si_3N_4 (3.2 nm effective thickness). The dotted line indicates the spectral position λ_{\max} of the absorbance maximum. (b) Corresponding SDRS spectra for different sputtering durations t_{sput} .

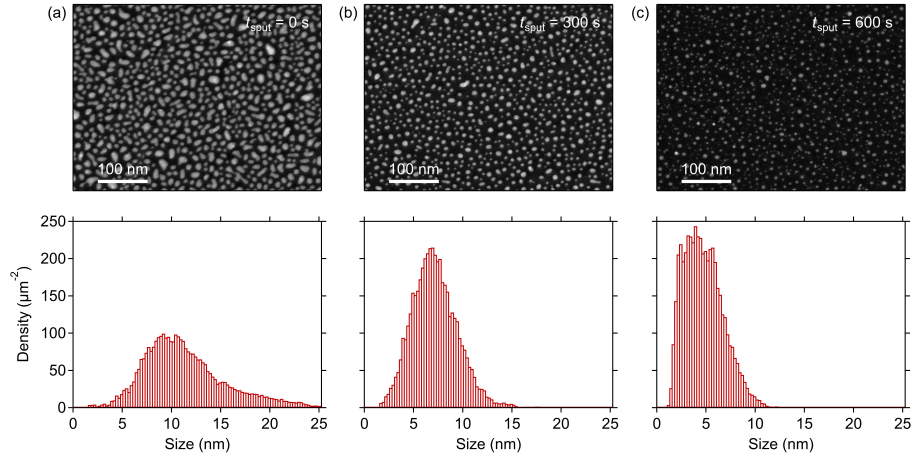


Figure S8: Plane-view HAADF-STEM images and corresponding nanoparticle size distributions for $\text{Si}_3\text{N}_4:\text{Ag}:\text{Si}_3\text{N}_4$ trilayers corresponding to different sputtering durations t_{sput} of an initially Ag nanoparticle layer (3.2 nm effective thickness) subjected to 80 eV Ar^+ -ion bombardment at normal incidence. (a) $t_{\text{sput}} = 0$ s, (b) $t_{\text{sput}} = 300$ s, and (c) $t_{\text{sput}} = 600$ s.